Hydrogen Permeation Characteristics of Melt-Spun Amorphous Alloy Membranes

S. Yamaura, H.M. Kimura, A. Inoue, M. Nishida*, Y. Shimpo* and H. Okouchi*

Institute for Materials Research, Tohoku Univ., Katahira 2-1-1, Aoba, Sendai 980-8577, Japan
Fax: 81-22-215-2137, e-mail: yamaura@imr.tohoku.ac.jp
*Fukuda Metal Foil & Powder Co. Ltd., Nishinoyama Nakatomicho 20, Yamashina, Kyoto 607-8305, Japan
Fax: 81-75-502-8928, e-mail: shinpo@fukuda-kyoto.co.jp

We examined the hydrogen permeation of the melt-spun $(Ni_{0.6}Nb_{0.4})_{100-x}Zr_x$ (x=0-50 at%) amorphous alloys. The maximum hydrogen permeability obtained in this work was 1.59×10^{-8} $mol \cdot m^{-1} \cdot s^{-1} \cdot Pa^{-1/2}$ at 673 K for the $(Ni_{0.6}Nb_{0.4})_{50}Zr_{50}$ amorphous alloy. It is noticed that the permeability is higher than that of pure Pd metal. Moreover, it was found that the permeability of the alloys prepared in this work was strongly affected by the amorphous local structural features inferred from the XRD observation. On the basis of these findings, the importance of optimization of the alloy composition is discussed.
Key words: hydrogen, membrane, permeation, separation, amorphous, melt-spinning, Ni-Nb-Zr alloy

1. INTRODUCTION

Nowadays, the Pd-Ag alloy membranes have been practically used for hydrogen purification for decades [1]. However, since the Pd metal is extremely expensive, it is very important to search for a new alloy possessing good hydrogen permeability as high as the Pd-Ag alloy. The new alloy should not include the Pd metal so much and if possible, it should be a non-Pd-based alloy with a minimum Pd addition. So far, a lot of studies on the non-Pd-based hydrogen permeable membrane were performed. For example, it was reported that the V-Ni alloys possessed excellent hydrogen permeability as high as the Pd-Ag alloy [2]. However, the V-Ni alloy is easily subjected to severe hydrogen embrittlement.

Amorphous alloys are known to have higher mechanical strength [3] and more excellent corrosion-resistance [4] than crystalline ones. Moreover, it was reported that the amorphous alloys showed good immunity from hydrogen embrittlement relative to crystalline ones [5]. Hara et al. reported that the melt-spun Ni-Zr amorphous alloys had enough mechanical strength without suffering from hydrogen embrittlement during the measurement although hydrogen permeability of those alloys was much lower than that of the Pd-Ag alloy [6]. We have tried to develop a practical membrane with high permeability and with insignificant embrittlement by employing the Ni-Nb-Zr ternary system. In our previous work, we reported that we could produce the melt-spun $(Ni_{0.6}Nb_{0.4})_{70}Zr_{30}$ amorphous alloys with high hydrogen permeability of 1.3×10^{-8} $mol \cdot m^{-1} \cdot s^{-1} \cdot Pa^{-1/2}$ [7]. However, we could not measure hydrogen permeability of the alloys with Zr content higher than 40 at% presumably because of embrittlement of the alloys and the technical problem in the measurement. Recently, we modified the sample cell and the experimental procedure for hydrogen permeation measurement. So, the objective of this work is to measure hydrogen permeability of the melt-spun $(Ni_{0.6}Nb_{0.4})_{100-x}Zr_x$ (x≥40 at%) amorphous

alloys and to examine the relationship between hydrogen permeability and the local structural features of the amorphous alloys.

2. EXPERIMENTAL

$(Ni_{0.6}Nb_{0.4})_{100-x}Zr_x$ (x=40, 50, 60 at%) alloy ingots were prepared by arc-melting the mixture of pure metals in an Ar atmosphere. Melt-spun ribbons were produced by a single-roller melt-spinning equipment in an Ar atmosphere. The ribbons to measure the hydrogen permeation and the density were about 20 mm wide and 40 µm thick and to the measure mechanical properties, about 1.5 mm wide and 20 µm thick.

The amorphicity of the melt-spun ribbon specimens was investigated by X-ray diffractometry (CuKα, 40 kV, 30 mA, hereafter denoted as XRD). The tensile fracture strength was measured at a strain rate of 4.2×10^{-3} s^{-1} with an Instron-type testing machine. The hardness was also measured by a Vickers microhardness tester with a load of 100 g. And the density was measured by the Archimedean principle.

Pd thin film of about 0.1 µm in thickness was deposited on both sides of specimens by the sputtering technique as an active catalyst for hydrogen dissociation and recombination during permeation. Hydrogen permeation measurements were performed with a conventional gas-permeation technique in the temperature range of 573 to 673 K at the hydrogen pressure up to 0.3 MPa. Sample membranes were mounted in the gas-permeation cell. The diameter of the permeation area was 5 mm. Pure hydrogen gas was introduced to one side of a membrane and then the flow rate of effluent gas from the other side (permeate side) was measured by a mass flow meter.

3. RESULTS

3.1 Amorphicity and mechanical properties

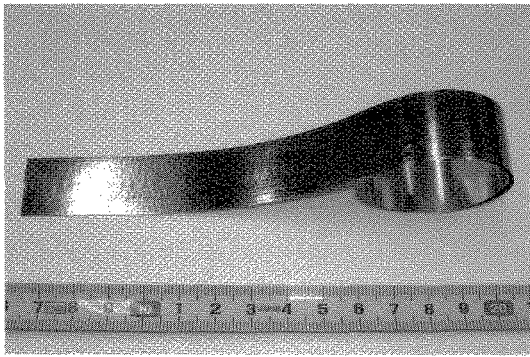Figure 1 shows the optical photograph of the melt-spun $(Ni_{0.6}Nb_{0.4})_{50}Zr_{50}$ ribbon. We had no problem

Fig.1 A photograph of the melt-spun $(Ni_{0.6}Nb_{0.4})_{50}Zr_{50}$ ribbon.
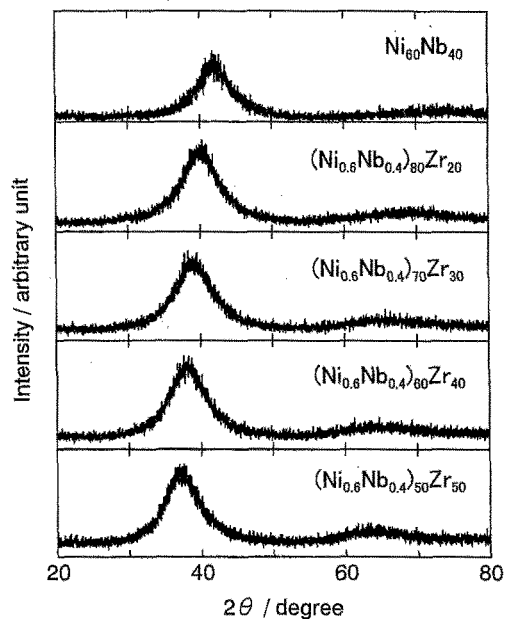

Fig.2 The X-ray diffraction patterns of the melt-spun $(Ni_{0.6}Nb_{0.4})_{100-x}Zr_x$ (x=0-50 at%) ribbons.

when producing rapidly solidified ribbons of the alloys prepared in this work by a conventional melt-spinning technique.

Figure 2 shows the XRD patterns of the melt-spun $(Ni_{0.6}Nb_{0.4})_{100-x}Zr_x$ (x= 50 at%) with previously reported patterns of x=0, 20, 30 and 40 at% by the present authors. No sharp diffraction peaks are seen in the 2θ range of 20-80°. This indicates that all alloys possess a single amorphous phase. Besides, a halo peak shifts to lower angles with increasing Zr content, indicating that the amorphous local structure is changed by Zr addition.

The result of measuring the tensile fracture strength is shown in Fig. 3(a) and the Vickers hardness in Fig. 3(b). As shown in the figures, both the tensile fracture strength and the Vickers hardness decrease with increasing Zr content. Kimura et al. reported that the thermal stability of the melt-spun Ni-Nb-Zr amorphous alloys also decreased with increasing Zr content [8]. Therefore, it may be difficult to adopt the Ni-Nb-Zr amorphous alloy with extremely large amount of Zr content as a hydrogen permeable membrane working at
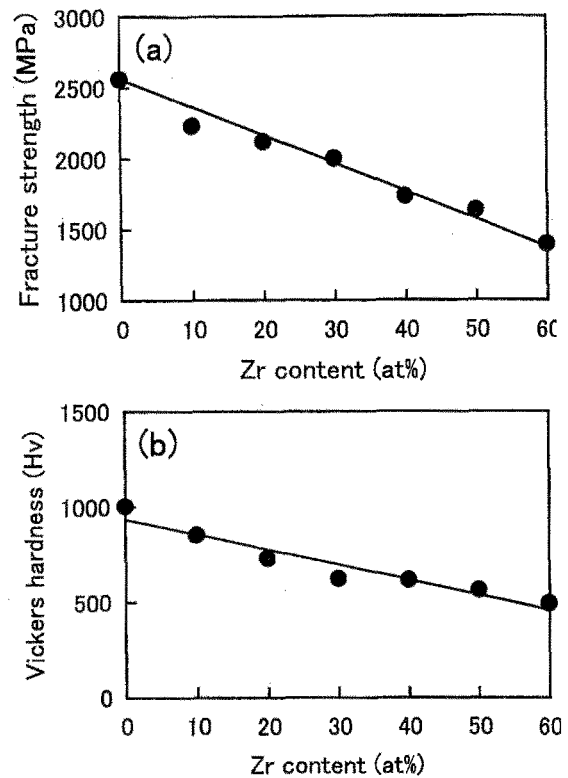

Fig.3 The mechanical properties of the melt-spun $(Ni_{0.6}Nb_{0.4})_{100-x}Zr_x$ (x=0-60 at%) ribbons. (a) the tensile fracture strength and (b) the Vickers hardness.

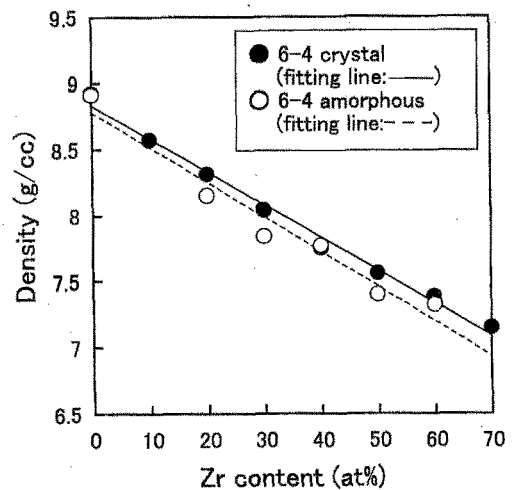Fig.4 The density of the $(Ni_{0.6}Nb_{0.4})_{100-x}Zr_x$ (x=0-70 at%) amorphous alloys and crystalline ones.

high temperature and high hydrogen pressure in practical use.

Figure 4 shows the density of both the crystalline and the amorphous alloys. The density of the crystalline alloys is measured with the arc-melted ingots of those alloys. It is natural that the crystalline alloys are denser than the amorphous ones. It is found that the density of both the crystalline and the amorphous alloys decreases with increasing Zr content. In the case of amorphous alloys, since the alloy density may be strongly affected

by the local packing structure, the decrease of the density may be related to the structural change, especially the increase in the interatomic distance in the amorphous alloy.

3.2 Hydrogen permeability

Figure 5 shows the hydrogen permeability of the melt-spun $(Ni_{0.6}Nb_{0.4})_{100-x}Zr_x$ (x= 40 and 50 at%) with previously reported data of x=0, 20, 30 at% by the present authors [7] and the wave vector, $K_p = (4\pi \cdot \sin\theta)/\lambda$ as a function of Zr content in the alloys, where θ is the angle of the halo peak position shown in Fig.2. It is shown that the permeability increases with decreasing the wave vector K_p value. The decrease in the K_p value indicates that the nearest neighbor distance of the atoms in the amorphous structure increases by Zr addition. It can be said from this observation that the amorphous alloy having a larger atomic spacing possesses higher hydrogen permeability in this alloy system. In this work, the highest permeation coefficient was 1.59×10^{-8} $mol \cdot m^{-1} \cdot s^{-1} \cdot Pa^{-1/2}$ at 673 K for the $(Ni_{0.6}Nb_{0.4})_{50}Zr_{50}$ amorphous alloy.
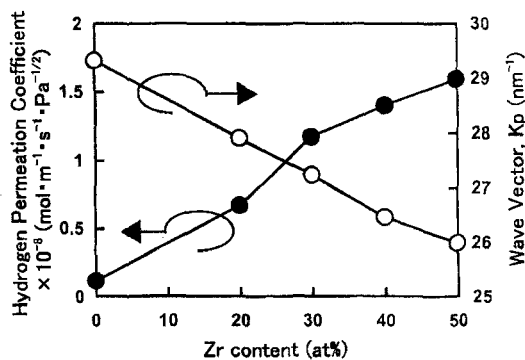

Fig.5 The hydrogen permeability and the wave vector as a function of Zr content in the alloys.

4. DISCUSSION

As shown in Fig.5, it is noticed that the hydrogen permeability of the $(Ni_{0.6}Nb_{0.4})_{50}Zr_{50}$ amorphous alloy is larger than that of pure Pd metal (about 9.5×10^{-9} $mol \cdot m^{-1} \cdot s^{-1} \cdot Pa^{-1/2}$). These permeation characteristics indicate the possibility of future practical use of the melt-spun amorphous alloy as a hydrogen permeable membrane.

Moreover, we tentatively investigated the local structure of the melt-spun Ni-Nb-Zr amorphous alloys by the radial distribution analysis. From the analysis, we found that the number of Zr-Zr pairs in amorphous structure increased with increasing Zr content of the alloys. The Zr-Zr pair has the largest interatomic distance than any other atomic pairs such as Ni-Ni, Ni-Nb, Ni-Zr, Nb-Nb and Nb-Zr pairs. And we also found that there may be a tendency that the Zr atoms gather with each other and form a cluster of a few atoms which is much smaller than a nano-grain. Figure 6 shows a schematic illustration of an imaginary local atomic structure derived from this analysis and the consideration by the XRD observation. From these findings, we can conclude that the Zr atoms form a small cluster and the interatomic distance increases with

increasing Zr content. Hydrogen atoms can permeate through such small Zr regions, which results in the increase in hydrogen permeation.

However, the requirements the hydrogen permeable membranes have to meet are not only high hydrogen permeability but also excellent immunity from hydrogen embrittlement. When practically used in a severe atmosphere at high temperature and at high hydrogen pressure, a membrane would absorb much hydrogen, which causes a volume expansion, and then collapses due to hydrogen embrittlement. In the case of the amorphous alloys prepared in this work, although hydrogen atoms can pass through the Zr region and probably can swell the Zr region at the same time, the Ni-Nb alloy region which has relatively small interaction with hydrogen, would play a role of a buffer phase to prevent the collapse of the Zr region.

As shown in Fig.5, hydrogen permeability may be improved by the Zr addition more than 50 at%. However, the permeability may be saturated to a certain level if the average interatomic distance becomes enough large. And too much addition of Zr atoms in the alloys cause significant embrittlement induced by hydrogen absorption. Therefore, we need to find the optimum composition with high hydrogen permeability and excellent immunity from hydrogen embrittlement.
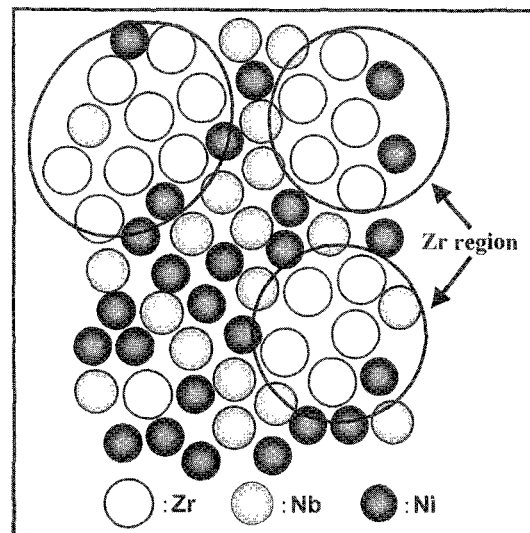

Fig.6 A schematic illustration of a model of local atomic structure derived from the XRD observation

5. SUMMARY

The conclusions of this work are summarized as follows;
(1) Fracture strength and Vickers hardness of the alloys decrease with increasing Zr content.
(2) A halo peak shifts to lower angles and the related K_p value decreases with increasing Zr content. And the density of the alloys also decreases with increasing Zr content. From these observations, it is estimated that the average interatomic distance in the amorphous local structure may increase with increasing Zr content in the alloys.
(3) Since Zr atoms can easily gather with each other, which results in the increase in the number of the "path" along which H atoms can easily permeate, hydrogen permeability increased with increasing Zr content. The

maximum permeation coefficient was 1.59×10^{-8} $mol \cdot m^{-1} \cdot s^{-1} \cdot Pa^{-1/2}$ at 673 K for the $(Ni_{0.6}Nb_{0.4})_{50}Zr_{50}$ amorphous alloy in this work.

6. ACKNOWLEDGMENT

References

[1] C. Hsu and R.E. Buxbaum, *J. Nucl. Mater.*, **141-143**, 238-243 (1986).

[2] C. Nishimura, M. Komaki, S. Hwang and M. Amano, *J. Alloy. Comp.*, **330-332**, 902-906 (2002).

[3] A. Inoue, *Mater. Trans., JIM*, **36**, 866-875 (1995).

[4] M. Naka, K. Hashimoto and T. Masumoto, *J. Non-Cryst. Sol.*, **30**, 29-36 (1978).

[5] S. Yamaura, M. Hasegawa, H.M. Kimura and A. Inoue, *Mater. Trans.*, **43**, 2543-2547 (2002).

[6] S. Hara, K. Sasaki, N. Itoh, H.M. Kimura, K. Asami and A. Inoue, *J. Membr. Sci.*, **164**, 289-294 (2000).

[7] S. Yamaura, Y. Shimpo, H. Okouchi, M. Nishida, O. Kajita, H.M. Kimura and A. Inoue, *Mater. Trans.*, **44**, 1885-1890 (2003).

[8] H.M. Kimura, A. Inoue, S. Yamaura, K. Sasamori, M. Nishida, Y. Shimpo and H. Okouchi, *Mater. Trans.*, **44**, 1167-1171 (2003).